

Barrow Neurological Institute at St. Joseph's Hospital and Medical Center

Barrow - St. Joseph's Scholarly Commons

Neurobiology

6-18-2015

Î±7 And Î²2 Nicotinic Acetylcholine Receptor Subunits Form Heteromeric Receptor Complexes That Are Expressed In The Human Cortex And Display Distinct Pharmacological Properties

Morten Skott Thomsen

Ruud Zwart

Daniel Ursu

Majbrit Myrup Jensen

Lars Hageman Pinborg

See next page for additional authors

Follow this and additional works at: <https://scholar.barrowneuro.org/neurobiology>

Recommended Citation

Thomsen, Morten Skott; Zwart, Ruud; Ursu, Daniel; Jensen, Majbrit Myrup; Pinborg, Lars Hageman; Gilmour, Gary; Wu, Jie; Sher, Emanuele; and Mikkelsen, Jens Damsgaard, "Î±7 And Î²2 Nicotinic Acetylcholine Receptor Subunits Form Heteromeric Receptor Complexes That Are Expressed In The Human Cortex And Display Distinct Pharmacological Properties" (2015). *Neurobiology*. 438.
<https://scholar.barrowneuro.org/neurobiology/438>

This Article is brought to you for free and open access by Barrow - St. Joseph's Scholarly Commons. It has been accepted for inclusion in Neurobiology by an authorized administrator of Barrow - St. Joseph's Scholarly Commons. For more information, please contact molly.harrington@dignityhealth.org.

Authors

Morten Skott Thomsen, Ruud Zwart, Daniel Ursu, Majbrit Myrup Jensen, Lars Hageman Pinborg, Gary Gilmour, Jie Wu, Emanuele Sher, and Jens Damsgaard Mikkelsen

RESEARCH ARTICLE

$\alpha 7$ and $\beta 2$ Nicotinic Acetylcholine Receptor Subunits Form Heteromeric Receptor Complexes that Are Expressed in the Human Cortex and Display Distinct Pharmacological Properties

Morten Skøtt Thomsen^{1‡}, Ruud Zwart², Daniel Ursu², Majbrit Myrup Jensen¹, Lars Hageman Pinborg^{1,3}, Gary Gilmour², Jie Wu⁴, Emanuele Sher², Jens Damsgaard Mikkelsen^{1*}

1 Neurobiology Research Unit, University Hospital Copenhagen, Rigshospitalet, Copenhagen, Denmark, **2** Lilly Research Centre, Eli Lilly and Company Limited, Erl Wood Manor, United Kingdom, **3** Epilepsy Clinic, University Hospital Copenhagen, Rigshospitalet, Copenhagen, Denmark, **4** Divisions of Neurology, Barrow Neurological Institute, St. Joseph's Hospital and Medical Center, Phoenix, United States of America

‡ Current address: Department of Drug Design and Pharmacology, Faculty of Health and Medical Sciences, University of Copenhagen, Copenhagen, Denmark

* jdm@nru.dk



CrossMark
click for updates

OPEN ACCESS

Citation: Thomsen MS, Zwart R, Ursu D, Jensen MM, Pinborg LH, Gilmour G, et al. (2015) $\alpha 7$ and $\beta 2$ Nicotinic Acetylcholine Receptor Subunits Form Heteromeric Receptor Complexes that Are Expressed in the Human Cortex and Display Distinct Pharmacological Properties. PLoS ONE 10(6): e0130572. doi:10.1371/journal.pone.0130572

Academic Editor: Huibert D. Mansvelder, Neuroscience Campus Amsterdam, VU University, NETHERLANDS

Received: January 16, 2015

Accepted: May 21, 2015

Published: June 18, 2015

Copyright: © 2015 Thomsen et al. This is an open access article distributed under the terms of the [Creative Commons Attribution License](https://creativecommons.org/licenses/by/4.0/), which permits unrestricted use, distribution, and reproduction in any medium, provided the original author and source are credited.

Data Availability Statement: All relevant data are within the paper.

Funding: This work was supported by the Danish Strategic Research Council (COGNITO, JDM), the Lundbeck Foundation (JDM), Eli Lilly and Company through the Lilly Research Award Program (JDM). The funder Eli Lilly and Company provided support in the form of salaries for authors RZ, DU, GG & ES, but did not have any additional role in the study design,

Abstract

The existence of $\alpha 7 \beta 2$ nicotinic acetylcholine receptors (nAChRs) has recently been demonstrated in both the rodent and human brain. Since $\alpha 7$ -containing nAChRs are promising drug targets for schizophrenia and Alzheimer's disease, it is critical to determine whether $\alpha 7 \beta 2$ nAChRs are present in the human brain, in which brain areas, and whether they differ functionally from $\alpha 7$ nAChR homomers. We used α -bungarotoxin to affinity purify $\alpha 7$ -containing nAChRs from surgically excised human temporal cortex, and found that $\alpha 7$ subunits co-purify with $\beta 2$ subunits, indicating the presence of $\alpha 7 \beta 2$ nAChRs in the human brain. We validated these results by demonstrating co-purification of $\beta 2$ from wild-type, but not $\alpha 7$ or $\beta 2$ knock-out mice. The pharmacology and kinetics of human $\alpha 7 \beta 2$ nAChRs differed significantly from that of $\alpha 7$ homomers in response to nAChR agonists when expressed in *Xenopus* oocytes and HEK293 cells. Notably, $\alpha 7 \beta 2$ heteromers expressed in HEK293 cells display markedly slower rise and decay phases. These results demonstrate that $\alpha 7$ subunits in the human brain form heteromeric complexes with $\beta 2$ subunits, and that human $\alpha 7 \beta 2$ nAChR heteromers respond to nAChR agonists with a unique pharmacology and kinetic profile. $\alpha 7 \beta 2$ nAChRs thus represent an alternative mechanism for the reported clinical efficacy of $\alpha 7$ nAChR ligands.

data collection and analysis, decision to publish, or preparation of the manuscript.

Competing Interests: RZ, DU, GG & ES are employees of Eli Lilly and Company Limited, whose company partly funded this study. There are no patents, products in development or marketed products to declare. This does not alter the authors' adherence to all the PLOS ONE policies on sharing data and materials.

Introduction

Neuronal nicotinic acetylcholine receptors (nAChRs) are pentameric ligand-gated ion channels. A total of 11 nAChR subunits ($\alpha 2-7$, $\alpha 9-10$, and $\beta 2-4$) have been cloned from mammalian neuronal tissue [1]. Of these, the $\alpha 7$ and $\alpha 9$ subunits can form homomeric receptors when expressed in heterologous expression systems, whereas the others assemble into heteromeric structures containing various combinations of α and β subunits [2]. Different combinations of subunits yield nAChRs that differ considerably in their functional and pharmacological properties [1].

With regard to the $\alpha 7$ nAChR, several studies have reported cognitive deficits in $\alpha 7$ knock-out mice and procognitive effects of selective $\alpha 7$ nAChR agonists [3–5]. Further, genetic studies have implicated the *CHRNA7* gene in schizophrenia and Alzheimer's disease [6–10]. The $\alpha 7$ nAChR is therefore considered a promising drug target for the treatment of cognitive symptoms in patients with schizophrenia or Alzheimer's disease, and this has led to an intensive drug development effort to produce $\alpha 7$ nAChR selective agonists and positive allosteric modulators (reviewed in [11]).

This research is based on an assumption that the $\alpha 7$ -containing nAChRs in the brain are homomers [4,12,13]. However, $\alpha 7$ subunits have been demonstrated to co-assemble with $\beta 2$, $\beta 3$, and $\beta 4$ subunits, respectively, after heterologous expression in *Xenopus* oocytes, and the resulting heteromers are functionally different from $\alpha 7$ nAChR homomers [14–19]. Furthermore, $\alpha 7$ and $\beta 2$ subunits have been shown to co-immunoprecipitate from rodent tissue from the hippocampus and ventral diagonal band of Broca, but not from the ventral tegmental area [16,20], suggesting that $\alpha 7\beta 2$ nAChR heteromers are present and have a discrete distribution in the mammalian brain. Furthermore Moretti et al. recently demonstrated that $\alpha 7$ and $\beta 2$ nAChR subunits form complexes in post mortem samples of human basal forebrain [21]. Interestingly, in contrast to the homomeric receptor, heterologously expressed $\alpha 7\beta 2$ nAChR heteromers are highly sensitive to blockade by $A\beta_{1-42}$, suggesting that $\alpha 7\beta 2$ nAChRs may play a unique role in the neuropathology of Alzheimer's disease [16].

These studies suggest that the function and pharmacology of $\alpha 7$ -containing nAChRs in the brain may be more diverse than has previously been appreciated, and that the function of native $\alpha 7$ nAChRs may depend on multiple interaction partners [22]. Notably, the potential presence of $\alpha 7\beta 2$ nAChR heteromers in the human cortex may have a significant impact on the clinical efficacy of ligands targeting the $\alpha 7$ subunit to improve cognition.

The first aim of this study was therefore to determine if $\alpha 7$ and $\beta 2$ subunits coassemble in the human cortex using affinity purification with the highly selective $\alpha 7$ antagonist α -bungarotoxin (α -Bgt). Next, we studied potential differences in pharmacology and kinetics of $\alpha 7\beta 2$ compared to $\alpha 7$ nAChRs in *Xenopus* oocytes and HEK293 cells in response to several $\alpha 7$ nAChR ligands.

Experimental procedures

Tissue

Human temporal neocortical tissue was obtained from anterior temporal resections performed in patients with medically intractable temporal lobe epilepsy with hippocampal onset. The study was approved by the Ethical Committee in the Capital Region of Denmark (H-2-2011-104) and performed in accordance with the Declaration of Helsinki. Written informed consent was obtained from both patients before surgery.

The tissue was dissected and immediately frozen on dry ice and stored at -80°C until use. The tissue contained all layers of the neocortex included the underlying white matter. Two

separate specimens were used for the present studies (females aged 30 and 44). The neuropathological examinations of the neocortex from both patients were normal.

Mice deficient for the $\alpha 7$ or $\beta 2$ nicotinic receptor (C57BL/6 background) or KO, and wild type (WT) littermates were purchased from The Jackson Laboratories and bred at Virginia Commonwealth University. 8–12 weeks old male or female homozygous knockout and age- and sex-matched wild-type mice were sacrificed by decapitation and the brains dissected and stored at -80°C . Cortical tissue was dissected using a scalpel.

Chemicals

All chemicals to prepare the recording and Barth's solutions, as well as dimethyl sulfoxide, acetylcholine chloride (ACh), carbamylcholine chloride (carbachol) and choline chloride were obtained from Sigma-Aldrich (Poole, U.K.). Dihydro- β -erythroidine hydrobromide (DH β E), methyllycaconitine citrate (MLA), (\pm)-epibatidine, and PNU120596 were purchased from Tocris (Bristol, U.K.). Compound B ([R-N-(1-azabicyclo[2,2,2]oct-3-yl)(2-pyridyl)thiophene-2-carboxamide, previously also named as compound A) was synthesized at Eli Lilly & Co and had a purity greater than 95% [19].

Affinity purification using α -bungarotoxin

α -Bgt (Biotium, Hayward, CA) was dissolved to 2.22 mg/ml in PBS, pH 7.4 at 4°C for 72 hours after which it was coupled to PureProteome NHS Flexibind magnetic beads (Millipore, Billerica, MA) in a ratio of 1:1.6 (vol/vol) using the manufacturer's instructions. Successful coupling was confirmed by subsequent protein determination showing a substantial decrease in the protein content of the α -Bgt solution. Another batch of beads was processed in parallel, but with no α -Bgt in the PBS, as a negative control. The beads were incubated in 0.1% bovine serum albumin in PBS, pH 7.4 for 1 hour at 4°C prior to use.

The tissue was lysed in 1 ml lysis buffer (50 mM Tris, 50 mM NaCl, 5 mM EDTA, 5 mM EGTA, 10 $\mu\text{l/ml}$ protease inhibitor cocktail (Sigma-Aldrich, Brøndby, Denmark), pH 7.5) using a PT1200C polytron blender (Kinematica, Luzern, Switzerland) for 20 seconds. The lysate was centrifuged 30 minutes at $160,000 \times g$ at 20 – 22°C using an air-driven ultracentrifuge (Airfuge, Copenhagen, Denmark), and the supernatant was discarded. The pellet was resuspended in 1 ml lysis buffer containing 2% Triton X-100 by blending for 20 seconds, and incubated for 2 hours at 4°C on a rotor (15 rpm). Thereafter, the sample was centrifuged as above and the resulting supernatant used for affinity purification. Total protein content was determined using the Pierce 660nm Protein Assay (Thermo scientific, Rockford, IL) and 500–800 μg protein was incubated with 50 μl magnetic beads in a total volume of 1500 μl lysis buffer for 18–22 hours at 4°C on a rotor (15 rpm). When comparing affinity purification with homogenates from $\alpha 7^{+/+}$ and a mixture of $\alpha 7^{-/-}$ and $\beta 2^{-/-}$ mice, the mixture was 1:1 and had double the amount of total protein in order to have equal amounts of $\alpha 7$ and $\beta 2$ subunits. Subsequently, the beads were washed twice in 1 M NaCl, 8 mM Na_2HPO_4 , 2 mM NaH_2PO_4 , 0.5% Triton X-100, pH 7.5 and three times in 0.1 M NaCl, 8 mM Na_2HPO_4 , 2 mM NaH_2PO_4 , 0.5% Triton X-100, pH 7.5 and immediately processed for western blotting.

Western blotting

Samples were diluted in loading buffer (final concentration: 60 mM Tris, 10% (v/v) glycerol, 5% (v/v) mercaptoethanol, 2% (w/v) SDS, 0.025% (w/v) bromophenol blue, pH 6.8), incubated for 5 minutes at 95°C and submitted to gel electrophoresis using AnykD gels (Biorad, Hercules, CA), and blotted onto PVDF membranes (BioRad). Membranes were washed in TBS-T and blocked in TBS containing 5% (w/v) dry milk powder, which was also used for antibody

incubations. Incubation in primary antibody against $\alpha 4$ (1:100, sc-5591, Santa Cruz Biotechnology, Heidelberg, Germany), $\alpha 7$ (1:1000, ab23832, Abcam, Cambridge, UK), or $\beta 2$ (1:1,000, a gift from Dr. Cecilia Gotti, which we have characterized previously [23]) was performed overnight at 4°C on parafilm in a humidified container, followed by 3×10 minute washes in TBS-T and 1 hour incubation at 20–22°C in horseradish peroxidase-coupled secondary antibody (1:1,000, Dako, Glostrup, Denmark). After thorough washing in TBS-T, enhanced chemiluminescence Western blotting detection reagents (Western Lightning ECL Pro, Perkin Elmer, Waltham, MA) were used for signal detection and protein bands were visualized using a Chemidoc XRS system with Quantity One software (Biorad). Mean optical densities of bands were measured and their corresponding background measurement subtracted.

nAChR expression and two-electrode voltage clamp on *Xenopus* oocytes

Xenopus oocyte expression and electrophysiological recordings were performed as described before [24]. Briefly, stage V and VI *Xenopus* oocytes (*Xenopus* Express, Vernassal, France) were prepared using standard procedures. Human $\alpha 7$ and $\beta 2$ subunit cDNAs, ligated into the pcDNA3 (Invitrogen) expression vector, were dissolved in distilled water at a concentration of 0.1 mg/ml (spectrophotometric determinations). $\alpha 7$ cDNA or a mixture of $\alpha 7$ and $\beta 2$ cDNA at a 1:10 ratio was injected into the nuclei of oocytes in a volume of 18.2 nl/oocyte, using a Nanoject Automatic Oocyte Injector (Drummond, Broomall, PA). The total amount of cDNA injected per oocyte was kept constant at 2 ng. After injection, oocytes were incubated at 18°C for 3–5 days in a modified Barth's solution containing 88 mM NaCl, 1 mM KCl, 2.4 mM NaHCO_3 , 0.3 mM $\text{Ca}(\text{NO}_3)_2$, 0.41 mM CaCl_2 , 0.82 mM MgSO_4 , 15 mM Hepes and 5 mg/l neomycin, pH 7.6. Recordings were performed 3–5 days post-injection. Oocytes were placed in a 0.1 ml recording chamber and perfused with a recording solution (containing in mM: NaCl 150, KCl 2.8, Hepes 10, CaCl_2 1.8; MgCl_2 1.0; pH 7.2, adjusted with NaOH) at a rate of 10 ml/min.

Oocytes were impaled by two microelectrodes filled with 3 M KCl (0.5–2.0 M Ω) and voltage-clamped at –60 mV using a Geneclamp 500B amplifier and PCLAMP 6 software (Axon Instruments, CA, U.S.A.). Typically, traces were filtered at 100 Hz during recording and digitized at 500 Hz using the DigiData 1200 interface (Axon Instruments, CA). All experiments were carried out at room temperature. Agonist concentration-response curves were obtained by normalizing agonist-induced responses to control responses induced by 1 mM ACh (a near-maximum effective concentration at $\alpha 7$ as well as $\alpha 7\beta 2$ receptors). An interval of 2 minutes was allowed between agonist applications, as this was found to be sufficient to ensure reproducible recordings.

Concentration-response curves were fitted by a non-linear least-squares algorithm according to the equation:

$$i = i_{\max} / (1 + \{EC_{50} / [\text{conc}]\}^n) \quad (1)$$

in which i_{\max} is the maximum obtainable peak current, EC_{50} is the concentration of the agonist that elicits 50% of the maximum obtainable peak current, and n is the slope factor. Results are expressed as mean \pm standard error of the mean.

nAChR expression and patch clamp on transfected HEK-293 cells

Patch clamp experiments were performed on transiently transfected HEK-293 cells. Transfections were performed in 6 well plates by using Lipofectamine 2000 (Invitrogen, Paisley, UK), and 2 μg $\alpha 7$ or $\alpha 7\beta 2$ (1:10) plasmid, using the same plasmids as in the oocyte experiments.

RIC-3 was used in the transfection protocol in a ratio 1:1 with $\alpha 7$ or $\alpha 7 / \beta 2$ plasmid, (2 μg) in order to boost trafficking of $\alpha 7$ -containing nAChRs. Transfected cells were plated in 35 mm bottom glass dishes the day after transfection and used for whole-cell voltage-clamp recordings after 48h. During recordings, cells were continuously perfused in HEPES-buffered Tyrode's solution (HBTS, Invitrogen, Paisley, UK) containing (in mM): 135 NaCl, 5 KCl, 1.2 MgCl_2 , 2.5 CaCl_2 , 10 HEPES, 11 glucose (pH = 7.2). Cells were voltage-clamped in the whole-cell configuration at a holding potential of -60 mV with an AxoPatch 200A patch-clamp amplifier (Molecular Devices, Sunnyvale, CA, USA). Pipettes were pulled from borosilicate glass (Type GC150F-10, Harvard Apparatus, Kent, UK) using a commercial puller (Model P-87, Sutter Instruments, Novato, CA, USA) and had resistances between 2 and 4 $\text{M}\Omega$ when filled with pipette solution containing (in mM): 127 CsCl, 1 MgCl_2 , 4 MgATP, 10 EGTA, 10 HEPES, 10 NaCl (pH = 7.3). Current data were recorded at 10 kHz using a DA/AD interface (Digidata 1322A, Molecular Devices, Sunnyvale, CA, USA). Drugs were applied using a multichannel perfusion system (Model BPS-8, Scientifica, Uckfield, UK) positioned 150 μm away from the recorded cell and controlled by Clampex 9 software (Molecular Devices, Sunnyvale, CA, USA).

Single cell calcium imaging

Fluorescence-based calcium imaging experiments were performed as described before [25]. Briefly HEK-293 cells (European Collection of Cell Cultures, #85120602) were transfected using the transfection protocol specified above and plated at a density of 20×10^5 cells/ml (50 μl per well) on poly(D)-lysine/laminin-coated black-walled clear bottom 96-well plates (Corning, UK). Cells were loaded in the dark for 60 minutes at 22°C in HBTS containing 4 μM of the calcium-sensitive dye Fluo-4 AM (Invitrogen, Paisley, UK) in the presence of 1% pluronic acid (Invitrogen). Cells were washed and continually perfused during the experiment with HBTS. Dye-loaded cells were viewed using an inverted epifluorescence microscope (Axiovert, 135TV, Zeiss, Cambridge, UK). Fluo-4 fluorescence was excited by a $480 \pm 10\text{nm}$ light source (Polychrome II, TILL-Photonics, Gräfelfing, Germany) and emission was captured by a iXon 897 EMCCD camera (Andor Technologies, Belfast, UK) after passage through a dichroic mirror (505LP nm) and a high pass barrier filter (515LP nm). Digitised images were stored and processed using Imaging Workbench 5.0 software (INDEC Biosystems, Santa Clara, CA, USA). Data were analysed by averaging individual traces collected from a large number of cells in multiple wells of the 96-well plate. Delta F/F0 values were measured by quantifying the ratio between the change in fluorescence signal intensity (delta F) and baseline fluorescence (F0).

Statistical analyses

Unpaired t-tests were used to compare time constants and log EC50 and IC50 values from *Xenopus* oocytes and peak currents in HEK293 cells. The statistical calculations were performed using GraphPad Prism version 6.03 for Windows (GraphPad Software, San Diego, USA). All data are presented as mean \pm standard error of the mean, and a *P*-value of less than 0.05 was considered statistically significant.

Results

$\alpha 7$ -containing nAChRs form heteromers with $\beta 2$ nAChR subunits in mouse cortex

We applied affinity purification using bead-coupled α -Bgt followed by Western blotting and antibody detection to detect $\alpha 7$ -containing nAChRs from extracts of mouse cortex. After isolation using bead-coupled α -Bgt, a 55 kDa protein band was readily detected from cortical

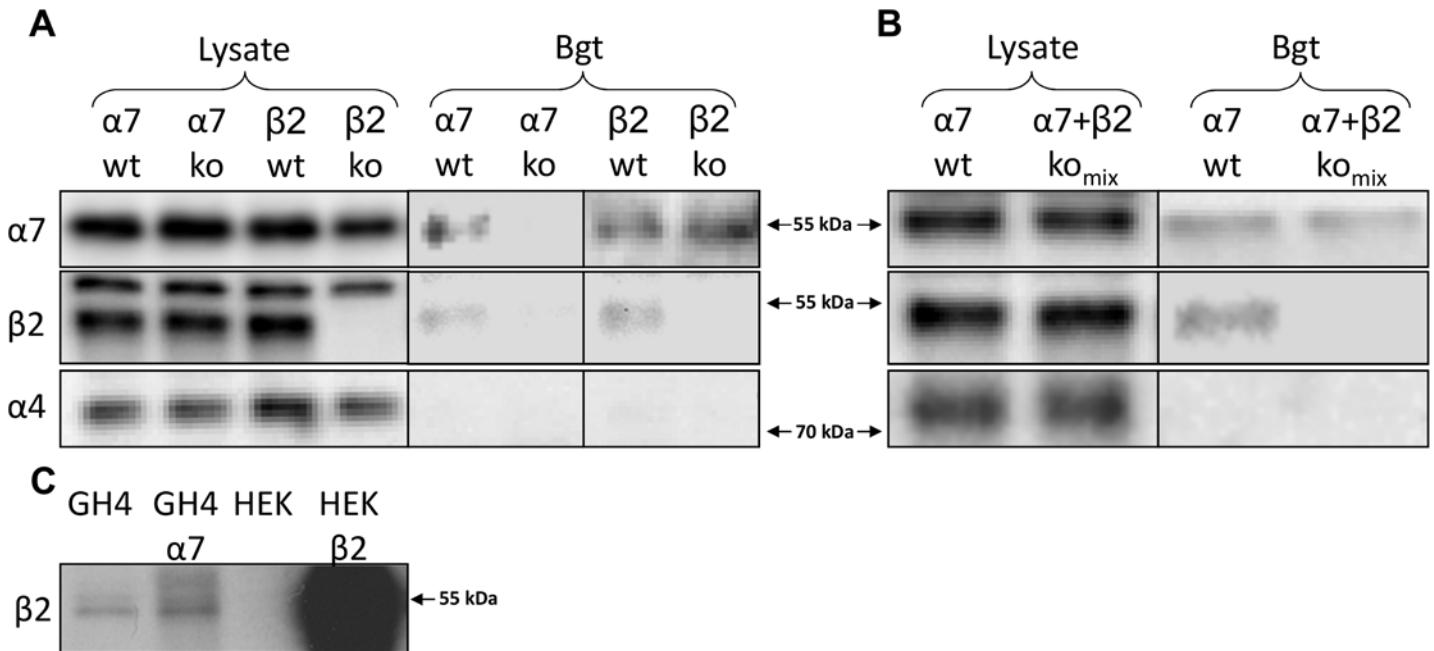


Fig 1. Bead-coupled α -bungarotoxin selectively purifies $\alpha 7$ -containing nAChRs from mouse cortex. (A) Affinity purification was performed with bead-coupled α -bungarotoxin (α -Bgt) on cortical homogenates from $\alpha 7^{+/+}$, $\alpha 7^{-/-}$, $\beta 2^{+/+}$, and $\beta 2^{-/-}$ mice and the isolated proteins were separated using gel electrophoresis. Subsequent detection using Western blotting demonstrated the presence of the $\alpha 7$ and $\beta 2$ in the isolates from $\alpha 7^{+/+}$ and $\beta 2^{+/+}$ mice. In isolates from $\alpha 7^{-/-}$ mice none of these proteins were detected, demonstrating that α -Bgt specifically isolates $\alpha 7$ -containing nAChRs, and that the detection of $\beta 2$ is dependent on the presence of $\alpha 7$ protein. In isolates from $\beta 2^{-/-}$ mice, there was no detection of $\beta 2$ protein, confirming the identity of the band isolated using α -Bgt as being $\beta 2$. The $\alpha 4$ subunit was not detected in any of the isolates, confirming that the presence of $\beta 2$ protein is not due to non-specific isolation of $\alpha 4\beta 2$ nAChRs. In the original tissue lysates $\alpha 7$, $\beta 2$, and $\alpha 4$ protein was readily detectable, except that $\beta 2$ is not detected in $\beta 2^{-/-}$ lysates, demonstrating the specificity of the antiserum. A 55 kDa protein was detected in both $\alpha 7^{+/+}$ and $\alpha 7^{-/-}$ lysates, as has previously been shown for several other $\alpha 7$ antibodies [26,27]. (B) α -Bgt affinity purification on cortical homogenates from $\alpha 7^{+/+}$ and a mixture of $\alpha 7^{-/-}$ and $\beta 2^{-/-}$ mice. $\beta 2$ subunits were not detected in the latter. (C) Detection of $\beta 2$ is evident in HEK293 cells transfected with the human $\beta 2$ gene (HEK $\beta 2$), but not in untransfected cells (HEK). Similarly transfection of GH4 cells with human $\alpha 7$ (GH4 $\alpha 7$) does not alter detection of the band corresponding to $\beta 2$.

doi:10.1371/journal.pone.0130572.g001

homogenates from $\alpha 7^{+/+}$, but not $\alpha 7^{-/-}$ mice. The absence of the band in $\alpha 7^{-/-}$ mice, clearly indicates that the band corresponds to the $\alpha 7$ protein, and thus demonstrates specific isolation of $\alpha 7$ -containing receptors using this approach (Fig 1A). The absence of a band corresponding to $\alpha 7$ protein in $\alpha 7^{-/-}$ mice also demonstrated the specificity of the used anti- $\alpha 7$ antibody in α -Bgt affinity purified samples. Without α -Bgt affinity purification, a 55 kDa protein band was readily detected in both $\alpha 7^{+/+}$ and $\alpha 7^{-/-}$ lysates, as previously shown for other $\alpha 7$ antisera [26,27]. This could be because the antibody used is raised against a part of the protein coded by exons 1–4, which are not deleted in the $\alpha 7^{-/-}$ mice, although binding of the antibody to other cellular targets sharing a similar epitope cannot be excluded [28]. Consequently, we were unable to determine the proportion of total $\alpha 7$ protein that was isolated by α -Bgt affinity purification.

We further showed that $\alpha 7$ -containing nAChRs isolated from the cortex of $\alpha 7^{+/+}$ and $\beta 2^{+/+}$ mice using bead-coupled α -Bgt co-purified with $\beta 2$ nAChR subunits (Fig 1A). No $\beta 2$ -immunoreactivity was detected in purified extracts from $\alpha 7^{-/-}$ mice, confirming that co-purification of $\beta 2$ only occurred in the presence of $\alpha 7$ protein. Similarly, no $\beta 2$ -immunoreactivity was detected in isolates from $\beta 2^{-/-}$ mice, confirming the identity of the band isolated using α -Bgt wild-type mice as being the $\beta 2$ subunit.

The $\beta 2$ antiserum immunoreacted with two separate bands around the expected molecular weight, but only the lower band was absent in $\beta 2^{-/-}$ lysates, demonstrating that this band

corresponds to the $\beta 2$ nAChR subunit. This band corresponded to the $\beta 2$ band observed in α -Bgt affinity purified samples. The $\alpha 4$ nAChR subunit was readily detectable in the original tissue lysates used for affinity purification, but was not detected in any of the isolates, suggesting that the presence of $\beta 2$ subunits is not due to non-specific isolation of $\alpha 4\beta 2$ -containing nAChRs.

Affinity purification performed with a 1:1 mixture of cortical homogenates from $\alpha 7^{-/-}$ and $\beta 2^{-/-}$ mice revealed no co-purification of $\beta 2$ nAChR subunits (Fig 1B).

To confirm that the $\beta 2$ antibody did not detect the $\alpha 7$ subunit, we demonstrate that transfection of GH4 cells with human $\alpha 7$ does not alter detection of the band corresponding to $\beta 2$, whereas expression of $\beta 2$ in HEK cells is readily detectable (Fig 1C).

$\alpha 7$ -containing nAChRs form heteromers with $\beta 2$ nAChR subunits in human cortex

We used the same affinity purification method to purify $\alpha 7$ -containing receptors from two human temporal cortex biopsies (Fig 2), and we were able to show co-purification of $\beta 2$ nAChR subunits with $\alpha 7$ in extracts from both human cortical biopsies. No bands were detected when performing the affinity purification with uncoupled beads, confirming that the isolation of $\alpha 7$ and $\beta 2$ was attributable to a specific interaction with α -Bgt.

No immunoreactivity for the $\alpha 4$ subunit was detected in any of the isolates, confirming that the presence of $\beta 2$ subunits is not due to non-specific isolation of $\alpha 4\beta 2$ -containing nAChRs.

$\alpha 7\beta 2$ nAChRs display different pharmacology from $\alpha 7$ nAChRs in *Xenopus* oocytes

When human $\alpha 7$ nAChR cDNA was expressed in oocytes, rapid activation and desensitization within about a second back to baseline was observed upon application of 1 mM ACh. Similarly, the selective $\alpha 7$ nAChR partial agonist compound B [25] at 100 μ M evoked a rapidly activated inward current that also completely desensitized back to baseline (Fig 3A). In oocytes expressing both $\alpha 7$ and $\beta 2$ nAChR subunits, 1 mM ACh induced a rapidly activating inward current that desensitized back to baseline, but the peak current responses were smaller and the speed of desensitization was slower than that of $\alpha 7$ homomers (Fig 3B). Compound B at 100 μ M also induced a rapidly activating inward current, but again the $\alpha 7\beta 2$ nAChR-mediated response were smaller and desensitized slower than that of $\alpha 7$ homomers. When fitted to a mono-exponential function,

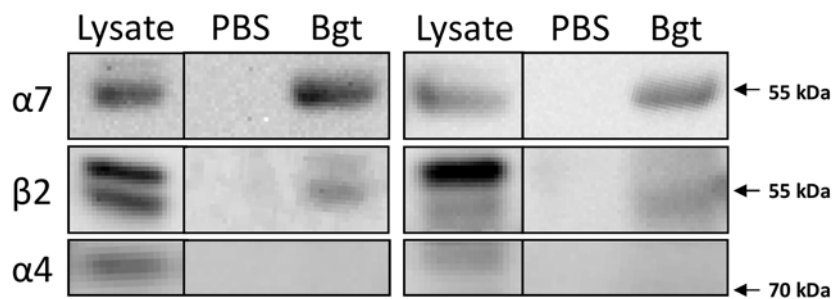


Fig 2. $\alpha 7$ -containing nAChRs form heteromers with $\beta 2$ nAChR subunits in human cortex. Magnetic beads covalently coupled with α -bungarotoxin (α -Bgt) or uncoupled beads (PBS) were incubated with homogenates from human temporal cortex (two separate identical experiments are shown) and the isolated proteins were separated using gel electrophoresis. Subsequent detection Western blotting demonstrated the presence of the $\alpha 7$ and $\beta 2$ from samples isolated using α -Bgt-coupled, but not uncoupled beads. The $\alpha 4$ subunit was not detected in any of the isolates, confirming that the presence of $\beta 2$ protein is not due to non-specific isolation of $\alpha 4\beta 2$ nAChRs.

doi:10.1371/journal.pone.0130572.g002

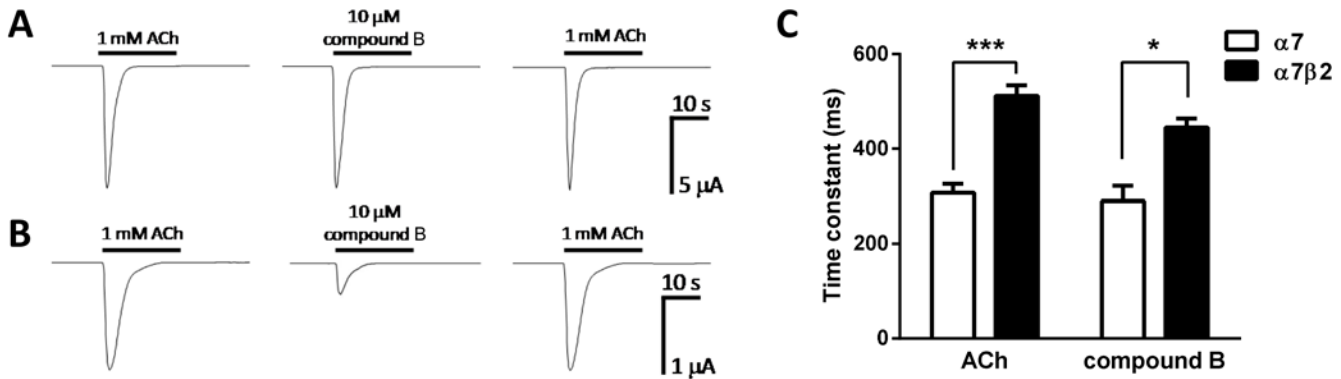


Fig 3. Responses of human $\alpha 7$ and $\alpha 7\beta 2$ nAChRs to the nAChR agonists acetylcholine (ACh) and compound B in *Xenopus* oocytes. A) 1 mM ACh and 100 μ M compound B evoke rapidly activating and desensitizing inward currents in oocytes expressing human $\alpha 7$ nAChRs. B) 1 mM ACh and 100 μ M compound B evoke rapidly activating and desensitizing inward currents in oocytes expressing human $\alpha 7\beta 2$ (1:10) nAChRs. C) Time constants for the decay phases of the responses to ACh (n = 6) and compound B (n = 3) for $\alpha 7$ and $\alpha 7\beta 2$ nAChRs when fitted to a mono-exponential function. *** $P < 0.001$ and * $P < 0.05$ indicates significant difference in an unpaired t-test.

doi:10.1371/journal.pone.0130572.g003

time constants for the decay phases of the responses to 1 mM ACh and 100 μ M compound B were significantly slower for $\alpha 7\beta 2$ compared to $\alpha 7$ nAChRs ($P < 0.001$ and $P < 0.05$, respectively, Fig 3C). The time constants of desensitization for both nAChR subtypes did not differ significantly depending on the agonist used.

Concentration-response curves for the two human receptors were measured for the agonists ACh, carbachol, choline, epibatidine, and compound B (Fig 4). Each concentration of agonist was applied for 2 seconds and peak current amplitudes were normalized to the average peak amplitude of a control 1 mM ACh induced current that were evoked before and after each concentration of test compound. Fitting the normalized responses to the Hill equation revealed that carbachol, choline and compound B had lower E_{max} in $\alpha 7\beta 2$ nAChRs compared to $\alpha 7$ nAChRs, and that epibatidine and compound B had significantly lower EC_{50} . Estimated parameters for EC_{50} , E_{max} , and slope factor are summarized in Table 1.

Similarly, concentration-response curves were also obtained for the antagonists DH β E and MLA (Fig 5). Various concentrations of antagonist were pre-applied for 1 min upon which it was co-applied with 1 mM ACh. Responses to 1 mM ACh in the presence of antagonist were normalized to the average of the 1 mM ACh-induced responses that were evoked before and after each antagonist application. Fitting the normalized responses to the Hill equation revealed that DH β E had significantly higher while MLA had significantly lower potency for $\alpha 7\beta 2$ compared to $\alpha 7$ nAChRs ($P < 0.01$ and $P < 0.05$, respectively).

One minute pre-application with 3 μ M of the $\alpha 7$ nAChR positive allosteric modulator PNU120596 resulted in a large potentiation of 1 mM ACh-induced response in an oocyte expressing h $\alpha 7$ nAChRs (2.5 ± 0.9 fold; n = 3, Fig 6A). 3 μ M PNU120596 also potentiated human $\alpha 7\beta 2$ nAChRs to a large extent (4.7 ± 2.8 fold; n = 3, Fig 6B), but this was not significantly different from the response to h $\alpha 7$ nAChRs.

$\alpha 7\beta 2$ nAChRs display different pharmacology from $\alpha 7$ nAChRs in HEK293 cells

Expression of $\alpha 7$ nAChRs in HEK293 cells was initially shown by using single cell calcium imaging responses to co-application of compound B and the $\alpha 7$ selective positive allosteric modulator PNU120596. (Fig 7A and 7B). As shown previously [29] co-expression of $\alpha 7$ with RIC-3 greatly enhanced the efficiency of the expression, as shown in our experiment by the

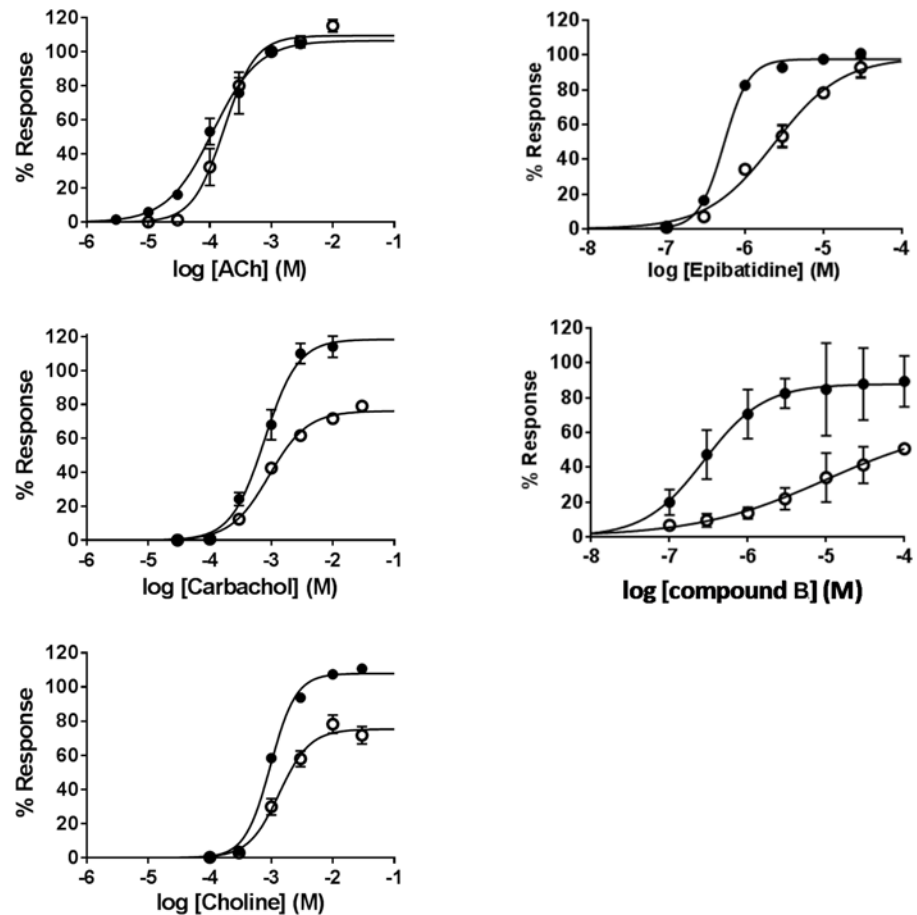


Fig 4. Concentration-response curves of nAChR agonists on human $\alpha 7$ and $\alpha 7\beta 2$ nAChRs in *Xenopus* oocytes. Acetylcholine (ACh), carbachol, choline, epibatidine and compound B were applied in various concentrations to *Xenopus* oocytes expressing $\alpha 7$ (filled circles) and $\alpha 7\beta 2$ (1:10, empty circles) nAChRs. All responses were normalized to the peak amplitude of a 1 mM control ACh-induced ion current in the respective oocyte.

doi:10.1371/journal.pone.0130572.g004

large increase in the number of responding cells ($44.9 \pm 0.8\%$ in the presence vs $3.3 \pm 0.3\%$ in the absence of RIC-3 respectively). Therefore, all subsequent experiments used RIC-3 as a co-expression cDNA. The amplitude of the agonist/modulator combination was very large while application of the compound B alone did not elicit any calcium fluxes. This is in agreement with previous studies [25] that showed that the transient nature of the $\alpha 7$ nAChR response is not sufficient to generate calcium fluxes that can be detected in this type of assay. We then compared directly the expression and relative response amplitudes of the $\alpha 7$ and $\alpha 7\beta 2$ (Fig 7C and 7D). Co-expression of $\alpha 7$ and $\beta 2$ caused a significant reduction in the number of responding cells (from $43.0 \pm 3.9\%$ to $8.4 \pm 1.6\%$). The reduction in expression efficacy was not caused by a decrease in the amplitude of responses induced by epibatidine (2.09 ± 0.09 and 2.32 ± 0.03 dF/F0 for $\alpha 7$ and $\alpha 7\beta 2$, respectively) or compound B (1.88 ± 0.04 and 2.08 ± 0.03 dF/F0, respectively) in the presence of the potentiator (Fig 7D).

When expressed in HEK293 cells $\alpha 7$ nAChRs rapidly activated upon application of $10 \mu\text{M}$ epibatidine and desensitized within about a second back to baseline. The selective $\alpha 7$ nAChR agonist compound B at $10 \mu\text{M}$ evoked a similar rapidly activated inward current that also completely desensitized to baseline (Fig 7E). In HEK293 cells expressing $\alpha 7\beta 2$ nAChRs $10 \mu\text{M}$

Table 1. Summary of agonist and antagonist concentration-response curves on human $\alpha 7$ and $\alpha 7\beta 2$ nAChRs expressed in *Xenopus oocytes*.

Agonist	$\alpha 7$				$\alpha 7\beta 2$ (1:10)				p
	EC50 (μM)	E _{max} (%)	nH	n	EC50 (μM)	E _{max} (%)	nH	n	
ACh	113 (78–163)	106 ± 6	1.17 ± 0.18	3	171 (138–211)	109 ± 3	1.70 ± 0.25	3	0.19
Carbachol	779 (598–1013)	118 ± 5	1.60 ± 0.25	3	923 (781–1090)	76 ± 2	1.39 ± 0.13	5	0.34
Choline	972 (888–1064)	108 ± 2	2.09 ± 0.19	3	1350 (1039–1755)	75 ± 4	1.74 ± 0.32	4	0.18
Epibatidine	0.54 (0.25–0.89)	98 ± 1	2.70 ± 0.13	4	(1.5–3.8)	99 ± 7	1.01 ± 0.15	3	0.046*
Comp. B	0.28 (0.15–0.51)	88 ± 5	1.14 ± 0.39	6	9.8 (4.9–19.6)	65 ± 21	0.53 ± 0.18	6	0.039*
Antagonist	IC50 (μM)	nH		n	2.4 IC50 (μM)	nH		n	
DH β E	47 (41–53)	2.74 ± 0.31		3	18 (14–23)	1.09 ± 0.14		3	0.003**
MLA	0.00089 (0.00074–0.00108)	1.69 ± 0.20		3	0.0013 (0.0011–0.0015)	1.60 ± 0.19		3	0.044*

All responses were normalized to the peak amplitude of a 1 mM control ACh-induced ion current. Antagonists were first pre-applied for 1 min followed by co-application with 1 mM ACh. During curve fitting of agonist data the bottom of the curves were constrained to 0 and curve fitting of antagonist data was performed by constraining the top and the bottom of the curves at 100 and 0%, respectively. T-tests on EC50 and IC50 data was performed on log EC50 and log IC50 values. Statistical significance

* $P < 0.05$

** $P < 0.005$.

doi:10.1371/journal.pone.0130572.t001

epibatidine induced a slowly activating inward current that reached a plateau before desensitizing. Compound B at 10 μM induced a very small slowly activating current with a very slow desensitization. Analysis of the peak currents normalized to the response to 10 μM epibatidine, revealed a much reduced current in response to compound B in $\alpha 7\beta 2$ compared with $\alpha 7$ transfected cells ($P < 0.05$, Fig 7F).

Discussion

We demonstrate that native human cortical $\alpha 7$ -containing nAChRs can form a complex with $\beta 2$ nAChR subunits. This is the first evidence for the presence of native $\alpha 7\beta 2$ nAChR heteromers in the human cortex. We further show that human $\alpha 7$ and $\alpha 7\beta 2$ nAChRs display marked pharmacological and kinetic differences in heterologous expression systems.

Previous studies have shown that $\alpha 7$ and $\beta 2$ nAChR subunits co-immunoprecipitate from the rat and mouse brain [16,20]. However, these studies employed $\alpha 7$ and $\beta 2$ antibodies that have been shown to stain knock-out tissue [26,27], which demands skepticism regarding co-immunoprecipitation results obtained using such antibodies. We used affinity purification with the highly selective $\alpha 7$ nAChR antagonist α -Bgt to determine that $\alpha 7$ and $\beta 2$ nAChR subunits co-purify from mouse cortex. We validated the method by showing that genetic ablation of either $\alpha 7$ or $\beta 2$ abolished this co-purification and by showing that $\alpha 4$ subunits were not co-purified, indicating that the co-purification of $\beta 2$ protein was not due to non-specific purification of $\alpha 4\beta 2$ nAChRs. To confirm that the $\alpha 7\beta 2$ complex occurred *in vivo*, we show that α -Bgt affinity purification on an extract containing tissue from both $\alpha 7^{-/-}$ and $\beta 2^{-/-}$ mice does not yield co-purification of $\beta 2$ subunits. We further demonstrated that the antibodies used for detection of $\alpha 7$ and $\beta 2$ nAChR subunits were specific under the conditions used.

Importantly, we were also able to demonstrate co-purification of $\alpha 7$ and $\beta 2$ nAChR subunits from human temporal cortex, indicating that native $\alpha 7\beta 2$ -containing nAChR heteromers are present in the human cortex. This finding complements a recent study demonstrating the existence of $\alpha 7\beta 2$ -containing nAChR heteromers in the human basal forebrain [21], and since the basal forebrain projects widely to the cortical mantle [30], this suggests that at least part of the $\alpha 7\beta 2$ nAChRs in the cortex might stem from cell bodies in the basal forebrain. Since α -Bgt

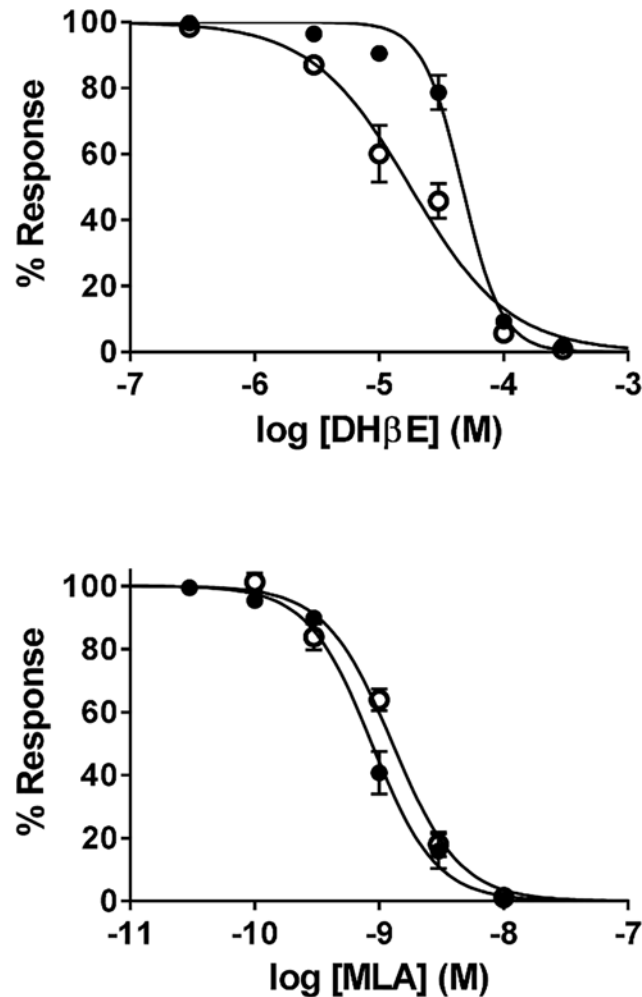


Fig 5. Effect of antagonists on human $\alpha 7$ and $\alpha 7\beta 2$ nAChRs in *Xenopus* oocytes. Inhibition curves for dihydro- β -erythroidine (Dh β E) and methyllycaconitine (MLA) on $\alpha 7$ (filled circles) and $\alpha 7\beta 2$ (1:10, empty circles) nAChRs. Co-expression of $\alpha 7\beta 2$ nAChR subunits lead to a significantly decreased IC₅₀ for Dh β E ($P < 0.01$), and an increased IC₅₀ for MLA ($P < 0.05$) compared to $\alpha 7$ nAChR homomers.

doi:10.1371/journal.pone.0130572.g005

binds to the interface between $\alpha 7$ subunits [31], we cannot use α -Bgt to detect protein from nAChR subunits that do not have $\alpha 7$ - $\alpha 7$ interfaces, i.e. receptors that contain one or two $\alpha 7$ subunits which are not adjacent in the receptor structure. Therefore, we cannot preclude the presence of other $\alpha 7$ -containing heteromeric nAChRs in addition to $\alpha 7\beta 2$ nAChRs.

Co-purification of subunits does not prove that the subunits form functional receptors, but the potential presence of functional $\alpha 7\beta 2$ nAChR heteromers in the human brain raises the possibility that compounds developed as selective ligands for $\alpha 7$ nAChR homomers may also affect heteromeric receptors in the human brain. To study the pharmacological consequences of incorporation of $\beta 2$ subunits into $\alpha 7$ -containing nAChRs, electrophysiological recordings were performed with human $\alpha 7$ and $\beta 2$ subunits expressed in *Xenopus* oocytes and HEK293 cells. In order to compare the present human $\alpha 7\beta 2$ nAChR data with previously reported rat $\alpha 7\beta 2$ nAChR data [15,19], we measured peak-amplitudes of agonist-induced ion currents rather than the net charge to create concentration-response curves. Peak responses and rate of desensitization for $\alpha 7\beta 2$ nAChR heteromers were generally lower than those of homomeric

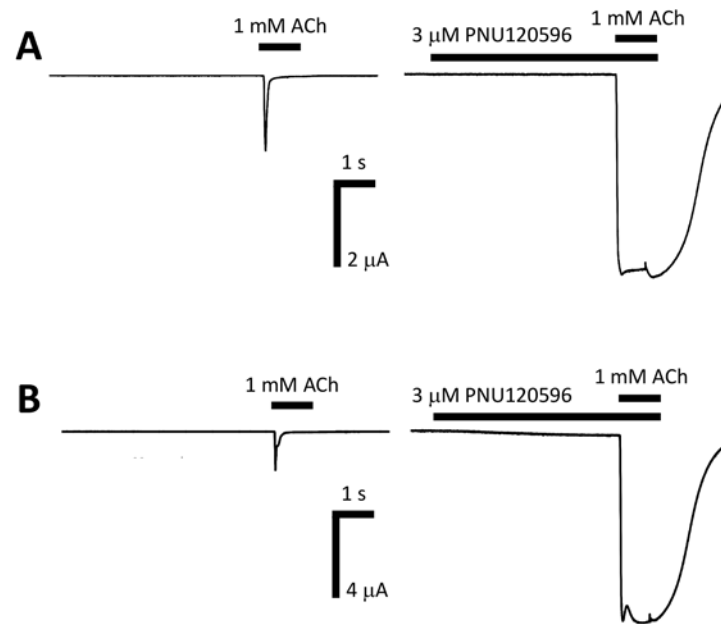


Fig 6. Potentiation of human $\alpha 7$ and $\alpha 7\beta 2$ nAChRs in *Xenopus* oocytes by the allosteric potentiator PNU120596. A) A control response was evoked by applying 1 mM ACh to an $\alpha 7$ nAChR expressing oocyte. After a 3 min wash period 3 μ M PNU120596 was applied to the same oocyte and after 1 min PNU120596 was co-applied with 1 mM ACh. In the presence of PNU120596 the peak of the 1 mM ACh-induced response was largely potentiated. B) A control response was evoked by applying 1 mM ACh to an $\alpha 7\beta 2$ nAChR expressing oocyte. After a 3 min wash period 3 μ M PNU120596 was applied to the same oocyte and after 1 min PNU120596 was co-applied with 1 mM ACh. In the presence of PNU120596 the peak of the 1 mM ACh response was largely potentiated.

doi:10.1371/journal.pone.0130572.g006

$\alpha 7$ nAChRs, which is in line with results from previous studies expressing mammalian $\alpha 7\beta 2$ nAChRs in oocytes [15,18,19]. Also in line with previous studies, the concentration-response curve for ACh was similar for human $\alpha 7\beta 2$ and $\alpha 7$ nAChRs, whereas the full $\alpha 7$ agonists carbachol and choline were only partial agonists on $\alpha 7\beta 2$ nAChRs.

Furthermore, the selective $\alpha 7$ partial agonist compound B had a lower efficacy at $\alpha 7\beta 2$ compared to $\alpha 7$ nAChRs, whereas the non-selective nAChR ligand epibatidine was a full agonist on both $\alpha 7\beta 2$ and $\alpha 7$ nAChRs. Similar results have been shown with rat $\alpha 7\beta 2$ nAChRs [19], with two notable differences: compound B has much higher efficacy on human compared to rat $\alpha 7\beta 2$ nAChRs, and the concentration-response curves for compound B and epibatidine on human $\alpha 7\beta 2$ nAChRs were less steep than observed with rat $\alpha 7\beta 2$ nAChRs, resulting in an increased EC_{50} [19].

Co-expression of $\alpha 7\beta 2$ nAChR subunits lead to a decreased IC_{50} of the $\alpha 4\beta 2$ preferring antagonist DH β E in *Xenopus* oocytes, which corroborates that $\beta 2$ subunits are incorporated into $\alpha 7$ -containing nAChRs. The IC_{50} of MLA was slightly increased in $\alpha 7\beta 2$ nAChRs, which may be the result of a decreased number of binding sites compared to $\alpha 7$ homomers, due to the incorporation of $\beta 2$ subunits.

Since expression of nAChRs in *Xenopus* oocytes have several limitations, including the possible formation of different subunit stoichiometries, and a current contribution from calcium-dependent chloride channels [32,33], we also investigated the function of $\alpha 7$ versus $\alpha 7\beta 2$ nAChRs expressed in the mammalian cell line HEK293. In HEK293 cells, epibatidine exhibited similar peak response currents in $\alpha 7$ and $\alpha 7\beta 2$ nAChR expressing cells, which differs from the 5 fold difference seen in *Xenopus* oocytes, whereas $\alpha 7\beta 2$ nAChRs displayed a reduced current

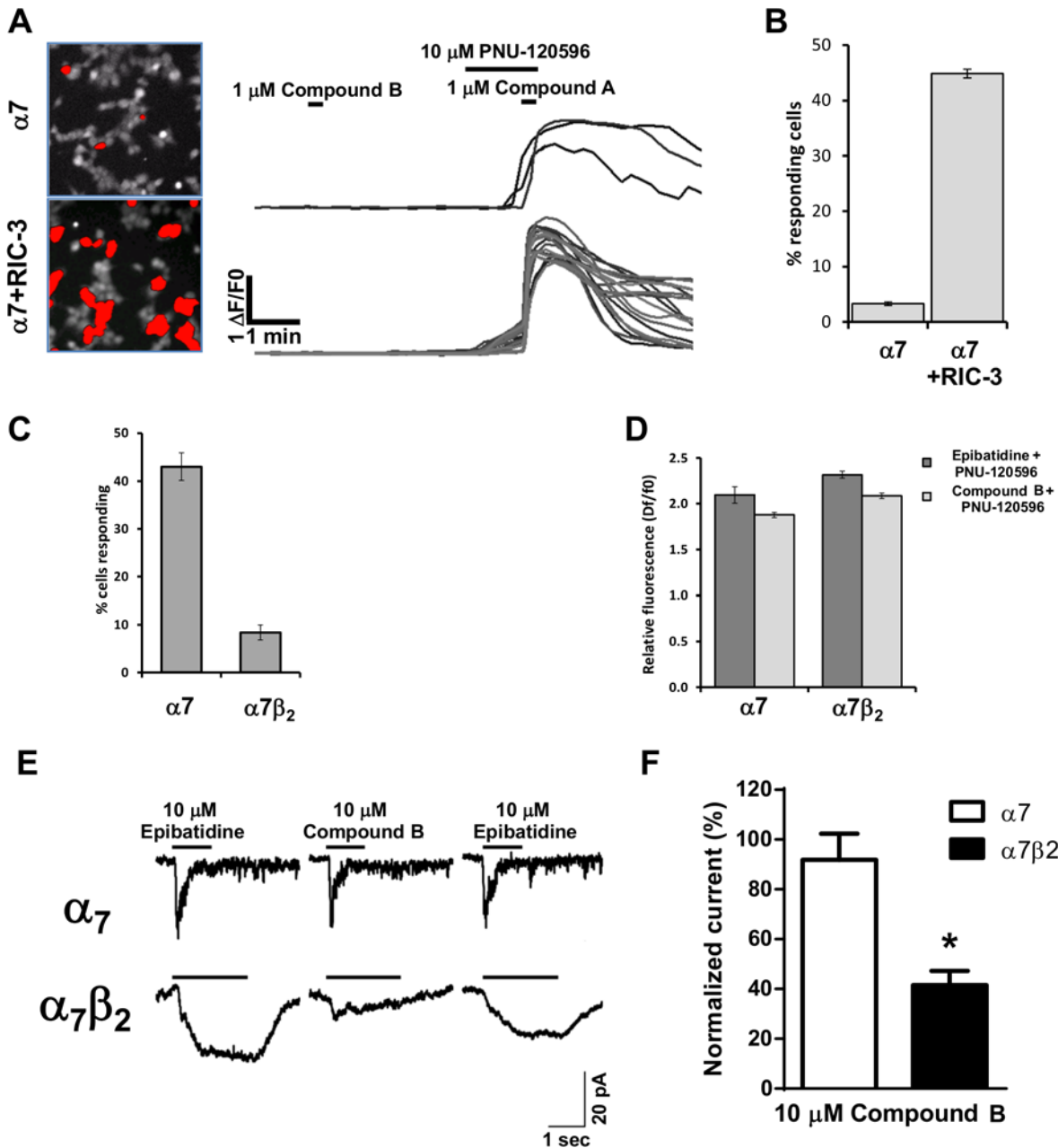


Fig 7. Responses of human $\alpha 7$ and $\alpha 7\beta 2$ nAChRs to the nAChR agonists epibatidine and compound B and the modulator PNU120596 in HEK293 cells. A) Efficiency of $\alpha 7$ expression was determined as the number of regions of interest (outlined in red in the left panel images) showing a fluorescence increase above a threshold of 0.1 $\Delta F/F_0$ following application of compound B and PNU-120596. Representative single cell traces are shown for the two transfection conditions with $\alpha 7$ alone and the combination of $\alpha 7$ and RIC-3. B) Relative expression efficiency for the experiment described in A. C) Expression efficiency in HEK293 cells transfected with either $\alpha 7$ or $\alpha 7\beta 2$ cDNA in the presence of RIC-3. D) The corresponding relative response amplitude for the two types of transfected cells obtained following co-application of either epibatidine (10 μM) or compound B (1 μM) and the $\alpha 7$ positive allosteric modulator PNU-120596 (10 μM). For data presented in panels A-D $n = 3$ for each experimental condition. E) Representative patch clamp recordings showing responses to the application of either epibatidine (10 μM) or compound B (10 μM) to cells expressing $\alpha 7$ (top traces) or $\alpha 7\beta 2$ (bottom trace) receptors. F) Averaged normalized data for the traces shown in E corresponding to 3 cells (out of 8 recorded for the $\alpha 7$ and 13 recorded for the $\alpha 7\beta 2$ transfected cells) that responded to the agonist application and were considered for analysis. Peak currents corresponding to application of compound B were normalised to the 1st epibatidine application. * $P < 0.05$ indicates significant difference in an unpaired t-test.

doi:10.1371/journal.pone.0130572.g007

response to compound B compared to $\alpha 7$ nAChR homomers. But more strikingly, the profile of the response to epibatidine and compound B was completely different in HEK293 cells compared to *Xenopus* oocytes. The $\alpha 7\beta 2$ nAChRs displayed a slow rise and decay phase, resulting in a very long response time, which was not seen with $\alpha 7$ homomers. These data demonstrate a much more pronounced kinetic difference between $\alpha 7\beta 2$ and $\alpha 7$ nAChRs than is evident when the receptors are expressed in *Xenopus* oocytes [18], and suggest that $\alpha 7\beta 2$ nAChRs in the human brain may display markedly different kinetics from $\alpha 7$ nAChR homomers. Importantly, the slow kinetics observed for $\alpha 7\beta 2$ may facilitate activation of Ca^{2+} -dependent intracellular signalling and neuronal excitability [34], suggesting that the $\alpha 7\beta 2$ nAChR may affect neuronal excitability to a much larger degree than $\alpha 7$ nAChR homomers. The number of responding HEK293 cells expressing $\alpha 7\beta 2$ was much lower compared to those expressing $\alpha 7$ nAChRs. This may reflect the fact that they expressed did not have $\alpha 7$ - $\alpha 7$ interfaces, which might be required for full activation of $\alpha 7\beta 2$ nAChR [18,21], or it could be due to potential dominant negative effects of $\beta 2$ presence on the assembly and trafficking of the receptors.

The $\alpha 7\beta 2$ -containing nAChRs constitute a particularly interesting molecular target for three main reasons: 1) $\alpha 7\beta 2$ nAChRs are found in the basal forebrain [16] where it has been shown that $\alpha 7$ and $\beta 2$ mRNA is co-expressed in the vast majority of the cholinergic cells [35]. Thus, modulation of $\alpha 7\beta 2$ nAChR heteromers offers the opportunity to selectively modulate activation of cholinergic neurons in the basal forebrain, which are important for attention and other cognitive functions [36]. 2) Nanomolar concentrations of $\text{A}\beta_{1-42}$ are able to block activation of $\alpha 7\beta 2$ nAChR heteromers, suggesting that this receptor may be uniquely affected in Alzheimer's disease [16,20]. 3) Compared with $\alpha 7$ homomers, the $\alpha 7\beta 2$ nAChR heteromers exhibit high sensitivity to volatile anaesthetics [37], suggesting that $\alpha 7\beta 2$ nAChR heteromers in the brain may be targets for anaesthetic action.

The presence of $\alpha 7\beta 2$ nAChR heteromers in the human cortex highlights the relevance of studying this receptor in relation to schizophrenia and Alzheimer's disease. However, such studies are hampered by the lack of $\alpha 7\beta 2$ nAChR selective compounds. All nAChR compounds tested so far display either unaltered or decreased current responses or EC_{50} on $\alpha 7\beta 2$ heteromeric compared to $\alpha 7$ homomeric nAChRs [15,18,19]. It has further been shown that for ACh, the $\beta 2$ subunits do not contribute to a binding site on the receptor, such that $\alpha 7\beta 2$ nAChR heteromers are only activated by their $\alpha 7$ - $\alpha 7$ interfaces [18]. Further efforts are necessary to reveal the impact of $\alpha 7\beta 2$ nAChR heteromers on cholinergic signalling in the brain, and whether novel agonists can activate these receptors through their $\alpha 7$ - $\beta 2$ interface(s). If possible, this would offer the exciting possibility of selective activating a distinct subpopulation of nAChRs in cholinergic cells, which may be important for cognitive function, and the function of which may be hampered in Alzheimer's disease.

In conclusion, we have demonstrated the presence of $\alpha 7\beta 2$ -containing heteromeric nAChRs in the human cortex. Future studies will reveal which brain regions and cell types contain these novel complexes as well as their physiological importance.

Acknowledgments

The authors would like to thank Maria Nørnberg for providing technical assistance, Dr. Imad Damaj for kindly providing tissue from transgenic mice (this tissue was the only mouse tissue used in our work), and Dr. Cecilia Gotti for kindly providing the $\beta 2$ antiserum.

Author Contributions

Conceived and designed the experiments: MST RZ DU GG ES JDM. Performed the experiments: MST RZ DU MMJ. Analyzed the data: MST RZ DU MMJ. Contributed reagents/materials/analysis tools: LHP. Wrote the paper: MST RZ JW JDM.

References

1. Albuquerque EX, Pereira EFR, Alkondon M, Rogers SW. Mammalian nicotinic acetylcholine receptors: from structure to function. *Physiol Rev.* 2009; 89: 73–120. doi: [10.1152/physrev.00015.2008](https://doi.org/10.1152/physrev.00015.2008) PMID: [19126755](https://pubmed.ncbi.nlm.nih.gov/19126755/)
2. Gotti C, Clementi F. Neuronal nicotinic receptors: from structure to pathology. *Prog Neurobiol.* 2004; 74: 363–96. doi: [10.1016/j.pneurobio.2004.09.006](https://doi.org/10.1016/j.pneurobio.2004.09.006) PMID: [15649582](https://pubmed.ncbi.nlm.nih.gov/15649582/)
3. Thomsen MS, Christensen DZ, Hansen HH, Redrobe JP, Mikkelsen JD. $\alpha 7$ Nicotinic acetylcholine receptor activation prevents behavioral and molecular changes induced by repeated phencyclidine treatment. *Neuropharmacology.* Elsevier Ltd; 2009; 56: 1001–1009. doi: [10.1016/j.neuropharm.2009.02.003](https://doi.org/10.1016/j.neuropharm.2009.02.003)
4. Lendvai B, Kassai F, Szájlí A, Némethy Z. $\alpha 7$ nicotinic acetylcholine receptors and their role in cognition. *Brain Res Bull.* Elsevier Inc.; 2013; 93: 86–96. doi: [10.1016/j.brainresbull.2012.11.003](https://doi.org/10.1016/j.brainresbull.2012.11.003) PMID: [23178154](https://pubmed.ncbi.nlm.nih.gov/23178154/)
5. Brooks JM, Pershing ML, Thomsen MS, Mikkelsen JD, Sarter M, Bruno JP. Transient inactivation of the neonatal ventral hippocampus impairs attentional set-shifting behavior: reversal with an $\alpha 7$ nicotinic agonist. *Neuropsychopharmacology.* 2012; 37: 2476–86. doi: [10.1038/npp.2012.106](https://doi.org/10.1038/npp.2012.106) PMID: [22781844](https://pubmed.ncbi.nlm.nih.gov/22781844/)
6. Stephens SH, Logel J, Barton A, Franks A, Schultz J, Short M, et al. Association of the 5'-upstream regulatory region of the $\alpha 7$ nicotinic acetylcholine receptor subunit gene (CHRNA7) with schizophrenia. *Schizophr Res.* 2009; 109: 102–12. doi: [10.1016/j.schres.2008.12.017](https://doi.org/10.1016/j.schres.2008.12.017) PMID: [19181484](https://pubmed.ncbi.nlm.nih.gov/19181484/)
7. Freedman R, Coon H, Myles-Worsley M, Orr-Urtreger a, Olincy a, Davis A, et al. Linkage of a neurophysiological deficit in schizophrenia to a chromosome 15 locus. *Proc Natl Acad Sci U S A.* 1997; 94: 587–592. doi: [10.1073/pnas.94.2.587](https://doi.org/10.1073/pnas.94.2.587) PMID: [9012828](https://pubmed.ncbi.nlm.nih.gov/9012828/)
8. Leonard S, Gault J, Hopkins J, Logel J, Vianzon R, Short M, et al. Association of promoter variants in the $\alpha 7$ nicotinic acetylcholine receptor subunit gene with an inhibitory deficit found in schizophrenia. *Arch Gen Psychiatry.* 2002; 59: 1085–1096. doi: [10.1001/archpsyc.59.12.1085](https://doi.org/10.1001/archpsyc.59.12.1085) PMID: [12470124](https://pubmed.ncbi.nlm.nih.gov/12470124/)
9. Carson R, Craig D, McGuinness B, Johnston JA, O'Neill FA, Passmore AP, et al. $\alpha 7$ nicotinic acetylcholine receptor gene and reduced risk of Alzheimer's disease. *Journal of medical genetics.* 2008. pp. 244–248. doi: [10.1136/jmg.2007.052704](https://doi.org/10.1136/jmg.2007.052704)
10. Carson R, Craig D, Hart D, Todd S, McGuinness B, Johnston J a, et al. Genetic variation in the $\alpha 7$ nicotinic acetylcholine receptor is associated with delusional symptoms in Alzheimer's disease. *Neuromolecular Med.* 2008; 10: 377–384. doi: [10.1007/s12017-008-8048-8](https://doi.org/10.1007/s12017-008-8048-8) PMID: [18696274](https://pubmed.ncbi.nlm.nih.gov/18696274/)
11. Thomsen MS, Hansen HH, Timmermann DB, Mikkelsen JD. Cognitive improvement by activation of $\alpha 7$ nicotinic acetylcholine receptors: from animal models to human pathophysiology. *Curr Pharm Des.* 2010; 16: 323–43. PMID: [20109142](https://pubmed.ncbi.nlm.nih.gov/20109142/)
12. Chen D, Patrick JW. The α -bungarotoxin-binding nicotinic acetylcholine receptor from rat brain contains only the $\alpha 7$ subunit. *J Biol Chem.* 1997; 272: 24024–9. PMID: [9295355](https://pubmed.ncbi.nlm.nih.gov/9295355/)
13. Drisdell RC, Green WN. Neuronal α -bungarotoxin receptors are $\alpha 7$ subunit homomers. *J Neurosci.* 2000; 20: 133–9. PMID: [10627589](https://pubmed.ncbi.nlm.nih.gov/10627589/)
14. Palma E, Maggi L, Barabino B, Eusebi F, Ballivet M. Nicotinic acetylcholine receptors assembled from the $\alpha 7$ and $\beta 3$ subunits. *J Biol Chem.* 1999; 274: 18335–40. PMID: [10373437](https://pubmed.ncbi.nlm.nih.gov/10373437/)
15. Khiroug SS, Harkness PC, Lamb PW, Sudweeks SN, Khiroug L, Millar NS, et al. Rat nicotinic ACh receptor $\alpha 7$ and $\beta 2$ subunits co-assemble to form functional heteromeric nicotinic receptor channels. *J Physiol.* 2002; 540: 425–434. doi: [10.1113/jphysiol.2001.013847](https://doi.org/10.1113/jphysiol.2001.013847) PMID: [11956333](https://pubmed.ncbi.nlm.nih.gov/11956333/)
16. Liu Q, Huang Y, Xue F, Simard A, DeChon J, Li G, et al. A novel nicotinic acetylcholine receptor subtype in basal forebrain cholinergic neurons with high sensitivity to amyloid peptides. *J Neurosci.* 2009; 29: 918–929. doi: [10.1523/JNEUROSCI.3952-08.2009](https://doi.org/10.1523/JNEUROSCI.3952-08.2009) PMID: [19176801](https://pubmed.ncbi.nlm.nih.gov/19176801/)
17. Criado M, Valor LLM, Mulet J, Gerber S, Sala S, Sala F. Expression and functional properties of $\alpha 7$ acetylcholine nicotinic receptors are modified in the presence of other receptor subunits. *J Neurochem.* 2012; 123: 504–514. doi: [10.1111/j.1471-4159.2012.07931.x](https://doi.org/10.1111/j.1471-4159.2012.07931.x) PMID: [22913551](https://pubmed.ncbi.nlm.nih.gov/22913551/)
18. Murray TA, Bertrand D, Papke RL, George AA, Pantoja R, Srinivasan R, et al. $\alpha 7\beta 2$ Nicotinic Acetylcholine Receptors Assemble, Function, and Are Activated Primarily via Their $\alpha 7$ - $\alpha 7$ Interfaces. *Mol Pharmacol.* 2012; 81: 175–88. doi: [10.1124/mol.111.074088](https://doi.org/10.1124/mol.111.074088) PMID: [22039094](https://pubmed.ncbi.nlm.nih.gov/22039094/)

19. Zwart R, Strotton M, Ching J, Astles PC, Sher E. Unique pharmacology of heteromeric $\alpha 7\beta 2$ nicotinic acetylcholine receptors expressed in *Xenopus laevis* oocytes. *Eur J Pharmacol*. Elsevier; 2014; 726C: 77–86. doi: [10.1016/j.ejphar.2014.01.031](https://doi.org/10.1016/j.ejphar.2014.01.031)
20. Liu Q, Huang Y, Shen J, Steffensen S, Wu J. Functional $\alpha 7\beta 2$ nicotinic acetylcholine receptors expressed in hippocampal interneurons exhibit high sensitivity to pathological level of amyloid β peptides. *BMC Neurosci*. BMC Neuroscience; 2012; 13: 155. doi: [10.1186/1471-2202-13-155](https://doi.org/10.1186/1471-2202-13-155)
21. Moretti M, Zoli M, George AA, Lukas RJ, Pistillo F, Maskos U, et al. The Novel $\alpha 7\beta 2$ -nicotinic Acetylcholine Receptor Subtype is Expressed in Mouse and Human Basal Forebrain: Biochemical and Pharmacological Characterisation. *Mol Pharmacol*. 2014; 86: 306–317. doi: [10.1124/mol.114.093377](https://doi.org/10.1124/mol.114.093377) PMID: [25002271](https://pubmed.ncbi.nlm.nih.gov/25002271/)
22. Thomsen MS, Mikkelsen JD. The $\alpha 7$ nicotinic acetylcholine receptor complex: one, two or multiple drug targets? *Curr Drug Targets*. 2012; 13: 707–20. PMID: [22300038](https://pubmed.ncbi.nlm.nih.gov/22300038/)
23. Thomsen MS, Cinar B, Jensen MM, Lyukmanova EN, Shulepko M a, Tsetlin V, et al. Expression of the Ly-6 family proteins Lynx1 and Ly6H in the rat brain is compartmentalized, cell-type specific, and developmentally regulated. *Brain Structure and Function*. 17 Nov 2014: 1–12. doi: [10.1007/s00429-013-0611-x](https://doi.org/10.1007/s00429-013-0611-x)
24. Zwart R, De Filippi G, Broad L., McPhie G., Pearson K., Baldwinson T, et al. 5-Hydroxyindole potentiates human $\alpha 7$ nicotinic receptor-mediated responses and enhances acetylcholine-induced glutamate release in cerebellar slices. *Neuropharmacology*. 2002; 43: 374–384. doi: [10.1016/S0028-3908\(02\)00094-1](https://doi.org/10.1016/S0028-3908(02)00094-1) PMID: [12243767](https://pubmed.ncbi.nlm.nih.gov/12243767/)
25. Gill JK, Chatzidaki A, Ursu D, Sher E, Millar NS. Contrasting Properties of $\alpha 7$ -Selective Orthosteric and Allosteric Agonists Examined on Native Nicotinic Acetylcholine Receptors. *PLoS One*. 2013; 8. doi: [10.1371/journal.pone.0055047](https://doi.org/10.1371/journal.pone.0055047)
26. Herber DL, Severance EG, Cuevas J, Morgan D, Gordon MN. Biochemical and histochemical evidence of nonspecific binding of $\alpha 7$ nAChR antibodies to mouse brain tissue. *J Histochem Cytochem*. 2004; 52: 1367–1376. doi: [10.1369/jhc.4A6319.2004](https://doi.org/10.1369/jhc.4A6319.2004) PMID: [15385583](https://pubmed.ncbi.nlm.nih.gov/15385583/)
27. Moser N, Mechawar N, Jones I, Gochberg-Sarver A, Orr-Urtreger A, Plomann M, et al. Evaluating the suitability of nicotinic acetylcholine receptor antibodies for standard immunodetection procedures. *J Neurochem*. 2007; 102: 479–492. doi: [10.1111/j.1471-4159.2007.04498.x](https://doi.org/10.1111/j.1471-4159.2007.04498.x) PMID: [17419810](https://pubmed.ncbi.nlm.nih.gov/17419810/)
28. Rommel FR, Raghavan B, Paddenberg R, Kummer W, Tumala S, Lochnit G, et al. Suitability of Nicotinic Acetylcholine Receptor 7 and Muscarinic Acetylcholine Receptor 3 Antibodies for Immune Detection: Evaluation in Murine Skin. *J Histochem Cytochem*. 2015; 1–11. doi: [10.1369/0022155415575028](https://doi.org/10.1369/0022155415575028)
29. Lansdell SJ, Gee VJ, Harkness PC, Doward AI, Baker ER, Gibb AJ, et al. RIC-3 enhances functional expression of multiple nicotinic acetylcholine receptor subtypes in mammalian cells. *Mol Pharmacol*. 2005; 68: 1431–1438. doi: [10.1124/mol.105.017459](https://doi.org/10.1124/mol.105.017459) PMID: [16120769](https://pubmed.ncbi.nlm.nih.gov/16120769/)
30. Zaborszky L, Csordas A, Mosca K, Kim J, Gielow MR, Vadasz C, et al. Neurons in the Basal Forebrain Project to the Cortex in a Complex Topographic Organization that Reflects Corticocortical Connectivity Patterns: An Experimental Study Based on Retrograde Tracing and 3D Reconstruction. *Cereb Cortex*. 2015; bht210. doi: [10.1093/cercor/bht210](https://doi.org/10.1093/cercor/bht210)
31. Harel M, Kasher R, Nicolas a, Guss JM, Balass M, Fridkin M, et al. The binding site of acetylcholine receptor as visualized in the X-Ray structure of a complex between α -bungarotoxin and a mimotope peptide. *Neuron*. 2001; 32: 265–275. doi: [S0896-6273\(01\)00461-5](https://doi.org/10.1016/S0896-6273(01)00461-5) [pii] PMID: [11683996](https://pubmed.ncbi.nlm.nih.gov/11683996/)
32. Krashia P, Moroni M, Broadbent S, Hofmann G, Kracun S, Beato M, et al. Human $\alpha 3\beta 4$ neuronal nicotinic receptors show different stoichiometry if they are expressed in *Xenopus* oocytes or mammalian HEK293 cells. *PLoS One*. 2010; 5: e13611. doi: [10.1371/journal.pone.0013611](https://doi.org/10.1371/journal.pone.0013611) PMID: [21049012](https://pubmed.ncbi.nlm.nih.gov/21049012/)
33. Papke RL, Smith-Maxwell C. High throughput electrophysiology with *Xenopus* oocytes. *Comb Chem High Throughput Screen*. 2009; 12: 38–50. PMID: [19149490](https://pubmed.ncbi.nlm.nih.gov/19149490/)
34. Berridge MJ. Neuronal calcium signaling. *Neuron*. 1998; 21: 13–26. doi: [10.1098/rstb.2008.0093](https://doi.org/10.1098/rstb.2008.0093) PMID: [9697848](https://pubmed.ncbi.nlm.nih.gov/9697848/)
35. Azam L, Winzer-Serhan U, Leslie F. M. Co-expression of $\alpha 7$ and $\beta 2$ nicotinic acetylcholine receptor subunit mRNAs within rat brain cholinergic neurons. *Neuroscience*. 2003; 119: 965–977. doi: [10.1016/S0306-4522\(03\)00220-3](https://doi.org/10.1016/S0306-4522(03)00220-3) PMID: [12831856](https://pubmed.ncbi.nlm.nih.gov/12831856/)
36. Hasselmo ME, Sarter M. Modes and models of forebrain cholinergic neuromodulation of cognition. *Neuropsychopharmacology*. Nature Publishing Group; 2011; 36: 52–73. doi: [10.1038/npp.2010.104](https://doi.org/10.1038/npp.2010.104) PMID: [20668433](https://pubmed.ncbi.nlm.nih.gov/20668433/)
37. Mowrey DD, Liu Q, Bondarenko V, Chen Q, Seyoum E, Xu Y, et al. Insights into distinct modulation of $\alpha 7$ and $\alpha 7\beta 2$ nicotinic acetylcholine receptors by the volatile anesthetic isoflurane. *J Biol Chem*. 2013; 288: 35793–800. doi: [10.1074/jbc.M113.508333](https://doi.org/10.1074/jbc.M113.508333) PMID: [24194515](https://pubmed.ncbi.nlm.nih.gov/24194515/)